Published in final edited form as:
Prostate. 2010 January 1; 70(1): 27–36. doi:10.1002/pros.21035.

Characterization of a novel novobiocin analogue as a putative C-terminal inhibitor of heat shock protein 90 in prostate cancer cells

B. Comer Shawna[1,#], **A. Vielhauer George**[2,#], **A. Manthe Craig**[1], **K. Chaguturu Vamsee**[2], **Szabla Kristen**[3], **L. Matts Robert**[3], **C. Donnelly Alison**[4], **S. J. Blagg Brian**[4], and **M. Holzbeierlein Jeffrey**[1,*]

[1]Department of Urology, University of Kansas Medical Center, Kansas City, KS

[2]University of Kansas Cancer Center, University of Kansas Medical Center, Kansas City, KS

[3]Department of Biochemistry and Molecular Biology, Oklahoma State University, Stillwater, Oklahoma

[4]Department of Medicinal Chemistry, University of Kansas, Lawrence, KS

Abstract

Purpose—Hsp90 is important in the folding, maturation and stabilization of pro-tumorigenic client proteins and represents a viable drug target for the design of chemotherapies. Previously, we reported the development of novobiocin analogues designed to inhibit the C-terminal portion of Hsp90, which demonstrated the ability to decrease client protein expression. We now report the characterization of the novel novobiocin analogue, F-4, which demonstrates improved cytotoxicity in prostate cancer cell lines compared to the N-terminal inhibitor, 17-AAG.

Materials and Methods—LNCaP and PC-3 cells were treated with 17-AAG or F-4 in anti-proliferative, apoptosis, cell cycle and cytotoxicity assays. Western blot and prostate specific antigen (PSA) ELISAs were used to determine client protein degradation, induction of Hsp90 and to assess the functional status of the androgen receptor (AR) in response to F-4 treatment. Surface Plasmon Resonance (SPR) was also used to determine the binding properties of F-4 to Hsp90.

Results—F-4 demonstrated improved potency and efficacy compared to novobiocin in anti-proliferative assays and decreased expression of client proteins. PSA secretion was inhibited in a dose-dependent manner that paralleled a decrease in AR expression. The binding of F-4 to Hsp90 was determined to be saturable with a binding affinity (K_d) of 100 μM. In addition, superior efficacy was demonstrated by F-4 compared to 17-AAG in experiments measuring cytotoxicity and apoptosis

Conclusions—These data reveal distinct modes of action for N-terminal and C-terminal Hsp90 inhibitors, which may offer unique therapeutic benefits for the treatment of prostate cancer.

Keywords

Hsp90 inhibitors; prostate cancer; novobiocin

[*]Address Correspondence to: Jeffrey M. Holzbeierlein, MD, Associate Professor of Urology, University of Kansas Medical Center, 3901 Rainbow Blvd, Mail Stop 1016, Kansas City, KS 66160.
[#]contributed equally

INTRODUCTION

Prostate cancer remains a significant health problem in the United States, responsible for 30,000 deaths annually, and is the second leading cancer killer of men (1). Patients with metastatic, locally recurrent, and androgen-independent prostate cancer are particularly problematic. Although recent trials demonstrate a modest survival advantage for docetaxel, the effectiveness of chemotherapy remains limited in these cases (2,3). Since prostate cancer is a heterogeneous disease with multiple contributing pathways, one strategy in the design of novel therapies is a focus on single agents with the ability to target multiple pathways.

Heat shock protein 90 (Hsp90) is a molecular chaperone responsible for folding nascent polypeptides into their biologically active conformations. In cancer, Hsp90 facilitates the conformational maturation of dormant oncogenic proteins important to tumorigenesis and cancer cell survival (4,5). Additionally, tumor cells exhibit higher Hsp90 activity and increased accumulation of Hsp90 inhibitors compared to normal cells, which may allow for the design of tumor-selective inhibitors (6,7). In contrast to traditional cancer therapeutics directed against one molecular target, disruption of the Hsp90 machinery may simultaneously inhibit multiple therapeutic targets and pathways critical to tumor survival. Thus, Hsp90 inhibitors represent an exciting new strategy in the development of prostate chemotherapies.

Traditionally, Hsp90 inhibitors have targeted the N-terminal ATP-binding site. Previous studies utilizing N-terminal inhibitors have demonstrated activity of these compounds *in vitro* and *in vivo*, and clinical trials are ongoing. Unfortunately, their use has been hampered by significant toxicity and problematic pharmacodynamic properties (8). More recently, a second ATP-binding site was identified in the carboxyl terminus of Hsp90 (9). Inhibition of the Hsp90 C-terminal ATP binding site decreases chaperone dimerization, diminishes ATPase activity and impairs formation of the Hsp90-client protein complex, resulting in improperly folded proteins that are targeted for the ubiquitin-proteasomal degradation pathway (10). The coumarin antibiotic novobiocin (NB) has been demonstrated to bind to the C-terminal ATP site of Hsp90 (11,12). Clinically, NB has been used for its antimicrobial activity with acceptable toxicity and bioavailability. Unfortunately, it exhibits a low affinity for Hsp90 with an IC_{50} of ~400 μM and would require high concentrations for maximal effects (11,12). Thus, we hypothesized that NB analogues with improved affinity for Hsp90 may represent effective therapy for prostate cancer. We have recently reported the synthesis and screening of NB analogues designed to bind to the Hsp90 C-terminal domain (11,13). Herein, we report the characterization of a novel analogue, F-4, in prostate cancer cell lines.

MATERIALS AND METHODS

Materials

NB analogues were synthesized as previously described (14). F-4 was dissolved in DMSO and stored at −20°C until use. Commercial antibodies were obtained for the androgen receptor (AR) (Cell Signaling Technologies, Danvers, MA), AKT, Hsp90, HER-2, and Actin (Santa Cruz Biotechnology Inc., Santa Cruz, CA), HIF-1α (Novus Biologicals, Littleton, CO), Hsp70 and GAPDH (Cell Signaling Technologies, Danvers, MA).

Cell culture

LNCaP (androgen-dependent) and PC-3 (androgen-independent) prostate cancer cell lines were obtained from American Type Culture Collection (Manassas, VA) and cultured in RPMI 1640 and Ham's F-12 media, respectively, with 10% FBS and penicillin/ streptomycin (100 IU/ml/ 100ug/ml) and maintained at 37°C with 5% CO_2.

Anti-proliferative assay

The CellTiter 96 AQueous One Solution Cell Proliferation Reagent (Promega) was used according to manufacturer protocol as previously described (15). Briefly, cell proliferation was measured by bioreduction of a tetrazolium (MTS) dye to a formazan by-product, which corresponds directly to viable cell number. Cells were incubated for 48 hours then treated for the indicated timepoints. Plates were analyzed on the VICTOR^{3}V Multilabel Reader (PerkinElmer) at 490 nm. Data was analyzed from 2–4 independent experiments performed in duplicate then normalized to absorbance of wells containing media only (0%) and untreated cells (100%). Non-linear regression and sigmoidal dose-response curves (GraphPad Prism) were used to calculate IC_{50}, IC_{90}, and R^2 values.

Trypan Blue cytotoxicity experiments

Cells were treated for the indicated timepoints then floating and adherent cells were collected. Each sample was mixed with equal parts Trypan Blue and analyzed on the VI-CELL Series Cell Viability Analyzer (Beckman Coulter, Fullerton, CA). Percentage of viable cells was calculated by determining the ratio of Trypan Blue-positive to negative cells.

Western Blot analysis

Western blot analysis was performed as previously described (16). Briefly, cells were treated with F-4 or vehicle (DMSO) for indicated times. Lysates were prepared, and equal amounts of protein were electrophoresed under reducing conditions on 4–12% Tris-Glycine gels (Invitrogen, Carlsbad, CA), transferred to a PVDF membrane (Millipore, Bedford, MA) then blocked in TBS-T containing 5% milk and probed with primary antibodies. Membranes were incubated with a horseradish peroxidase-conjugated secondary antibody, developed with chemiluminescence substrate (Pierce Biotechnology, Rockford, IL), and visualized with the UVP AutoChemi system (UVP, LLC, Upland, CA). All Western blots were probed for loading controls Actin or GAPDH. The data were representative of at least three independent experiments (n=3).

PSA ELISA assay

In vitro measurement of prostate specific antigen (PSA) secretion from LNCaP cells was assessed using the BioQuant PSA ELISA kit (BioQuant, Nashville, TN) according to manufacturer's instructions. Cells were cultured in medium containing 2% charcoal dextran-stripped serum for 3 days to reduce hormones to basal levels then treated with F-4 for 24 hours. Cells were either incubated with F-4 alone or in the presence of 100 nM testosterone (TST) for an additional 24 hours. Following incubation, samples of LNCaP-conditioned media were analyzed for PSA. Data was analyzed as described under **Anti-Proliferative Assay**. Data points represented the mean ± SEM of duplicate wells from four independent experiments (n=4).

Annexin V apoptosis experiments

Annexin V-FITC and propidium iodide (PI) (Anaspec, San Jose, CA) were prepared according to the manufacturer's instructions. Cells were treated, floating and adherent cells were collected, and the resulting cell suspension was washed in Annexin Binding Buffer (ABB) (150 μM NaCl, 5 μM KCl, 1 μM $MgCl_2{\cdot}6H_20$, 1.8 μM $CaCl_2{\cdot}2H_20$, 10 mM HEPES, and 2% FBS). Half the cell suspension was used for **Cell Cycle Analysis** (see below). The remaining cell suspension was stained with Annexin V-FITC (BD Pharmingen, San Jose, CA) and propidium iodide (Sigma Aldrich, St. Louis, MO) then washed and fixed in paraformaldehyde. Samples were analyzed using the BD LSRII System (BD Biosciences,

San Jose, CA) and were gated identically for all experiments. The data displayed represented the mean ± SEM of three independent experiments (n=3).

Cell cycle analysis

Cells were centrifuged and resuspended in 0.9% NaCl followed by drop-wise addition of 90% EtOH to fix cells. Samples were centrifuged then resuspended in PI followed by incubation with 1 mg/mL RNase A (Sigma Aldrich, St. Louis, MO). Samples were analyzed as described under Annexin V methods.

Statistical analysis

Data from **Annexin V apoptosis**, **cell cycle**, and **Trypan Blue** experiments were analyzed using a two-tailed t-test (GraphPad Prism 5.0, La Jolla, CA). All data displayed represented the mean ± SEM of at least three independent experiments (n=3).

Surface Plasmon Resonance (SPR) Analysis

Insect Sf9 cells overexpressing Hsp90β were cultured and harvested by the Baculovirus/Monoclonal Antibody Core facility at Baylor College of Medicine. Hsp90β was extracted and purified (>98% pure) as described previously(17,18), but without the initial DEAE-cellulose chromatography step. The surface of a SSOO COOH1 SPR sensor chip mounted in a SensiQ SPR instrument (ICX Nomadics) was activated by treatment with N-(3-dimethylaminopropyl)-N'-ethylcarbodiimide hydrochloride and N-hydroxysuccinimide for preferential cross-linking of the protein's N-terminus to the surface. For Hsp90 immobilization, 250 μL of Hsp90 (7 mg/ml) in 20 mM sodium bicarbonate buffer (pH 8) containing 150 mM NaCl was injected at a flow rate of 10 μL/min, giving 2800 response units of protein stably immobilized to surface of the flowcell, representing ~0.08 picomoles of Hsp90. Unreactive groups were then quenched with 1 M ethanolamine (pH 8), and the surface washed with buffer containing 10 mM PIPES pH 7.4, 300 mM NaCl, and 2% DMSO. F-4 was diluted in assay buffer containing 10 mM PIPES pH 7.4, 300 mM NaCl, and 2% DMSO and injected over the surface of the derivatized chip at a flow rate of 25 μL/min at 25°C at the indicated concentrations. All measurements were done in triplicate. SPR binding curves were analyzed using QDAT software (ICX Nomadics) to calculate the K_d and re-graphed using Origin software for Scatchard analysis and to demonstrate saturation of binding.

RESULTS

Anti-proliferative effects of F-4 in prostate cancer cell lines

The anti-proliferative effects of F-4, 17-AAG, and NB were examined over a 72 hour time-course in LNCaP and PC-3 cells (Figure 1). At all timepoints, F-4 dose-response curves were nearly superimposable with marginal improvement over time indicating that maximal efficacy (IC_{90}) and potency (IC_{50}) was essentially achieved at 24 hours (Table 1). Conversely, 17-AAG required at least 48–72 hours treatment to achieve superior efficacy and potency in both cell lines. F-4 was 14–24 fold and 7–9 fold more potent (IC_{50}) compared to the parent compound NB in the LNCaP and PC-3 cell lines, respectively, at all timepoints. These findings suggested that the NB analogue, F-4, required less time to exert its anti-proliferative effects compared to 17-AAG, which required 48–72 hours of continuous exposure to elicit maximal response.

Cytotoxicity of F-4 in prostate cancer cells

Since the previous assays in Figure 1 measure proliferation and not cytotoxicity, prostate cancer cells were examined to discern the relationship between anti-proliferative activity and

cytotoxicity. LNCaP (Figure 2, *top panels*) and PC-3 (Figure 2, *bottom panels*) cells were treated for 24 *(panels A & D)*, 48 *(panels B & E)*, or 72 *(panels D & F)* hours, and cell death was measured using the Trypan Blue exclusion assay. A dose-dependent increase in cell death was observed at concentrations of F-4 ranging from 25–50 μM and 50–100 μM in LNCaP and PC-3 cells, respectively. Additionally, 17-AAG was examined at concentrations ranging from 1–100 μM (highest dose shown) and only demonstrated appreciable cytotoxicity at the 100 μM dose following 72 hours treatment. Thus, these data demonstrate a strong correlation of the anti-proliferative effect of F-4 with its cytotoxic effects, whereas the potent anti-proliferative effect of 17-AAG reflects the cytostatic mechanism of the drug.

F-4 mediated degradation of client proteins

Client protein expression and subsequent degradation was examined in the LNCaP cell line treated with F-4 for 24 hours. Degradation of the HSP90 client proteins, AR, HER-2 and AKT, was observed in a dose-dependent manner (Figure 3A). HIF-1α protein levels were unaffected and the induction of Hsp90, a hallmark of HSP90 inhibition, was absent in F-4-treated LNCaP cells. The loading control Actin was marginally affected at the highest concentration.

In the PC-3 cell line, F-4 demonstrated degradation of the AKT and HER-2 proteins (Figure 3B) while Hsp90 expression was moderately increased following treatment with F-4 for 72 hours. HIF-1α levels appeared to be more sensitive to F-4-mediated client protein degradation, for which decreased expression was observed following 24 hours of treatment. These data demonstrate that F-4 triggers the degradation of client proteins, which is another hallmark of Hsp90 inhibition.

F-4 diminishes androgen-induced PSA secretion

PSA expression and secretion is regulated by androgens binding to their cognate androgen receptor (AR). Since F-4 decreases AR expression between 1–10 μM (Figure 3A), we examined the corresponding effect of F-4 on the secretion of PSA in the androgen-dependent LNCaP cells. Figure 4 demonstrates that treatment of LNCaP cells with testosterone alone results in a robust increase in PSA that was abrogated with pre-treatment of F-4. Furthermore, this was accomplished using drug concentrations previously shown to manifest the degradation of AR (see Figure 3). These data demonstrated that PSA levels can be utilized as a biomarker for assessing the effectiveness of C-terminal Hsp90 inhibitors in androgen-dependent prostate cancer.

F-4 manifests induction of apoptosis in prostate cancer cells

Induction of apoptosis was determined by Annexin V binding to externalized phosphatidylserine on the plasma membrane, and cell death was measured by propidium iodide staining. Treatment of prostate cancer cells with F-4 for 72 hours resulted in a dramatic dose-dependent induction of Annexin V staining compared to control (Figure 5A & 5C). Interestingly, the LNCaP cell line *(panel 5A)* appeared to undergo early-stage (quadrant IV) and late-stage (quadrant II) apoptosis that increased with dose while the less sensitive PC-3 cell line *(panel 5C)* was only observed to undergo early apoptosis (quadrant IV). Statistical analysis revealed a significant increase in total Annexin V staining at the 50 ($p<0.05$) and 100 μM ($p<0.01$) F-4 concentrations as compared to vehicle control (Figure 5B & 5D, *respectively*). Additionally, treatment of cells with a range of concentrations of 17-AAG (1–100 μM; highest dose shown) for 72 hours did not induce any appreciable Annexin V staining. These findings demonstrated F-4 to be more effective at inducing apoptosis in prostate cancer cells compared to 17-AAG.

Cell cycle effects of F-4 in prostate cancer cells

Cell cycle arrest, as determined by propidium iodide staining, was assessed in both prostate cancer cell lines following F-4 treatment. LNCaP cells revealed a marked increase in the sub-G0 percentage of cells ($p<0.01$) (Figure 6A) with a decrease in the percentage of cells in the G0/G1 *($p<0.05$)* and G2/M phase *($p<0.05$)* (Figure 6B). The sub-G0 peak represented cells undergoing apoptosis, characterized by the fragmentation and reduction in the amount of cellular DNA. Conversely, cell cycle analysis of PC-3 cells following exposure to F-4 resulted in a dose-dependent G2/M arrest *($p<0.05$)* (Figure 6C) with a corresponding decrease in the percentage of cells in the G0/G1 phase of the cell cycle *($p<0.05$)* (Figure 6D). Interestingly, treatment of both cell lines with a range of 17-AAG (1–100 μM; highest dose shown) resulted mainly in a G2/M arrest at all concentrations with mild induction of sub-G0 phase in only the LNCaP cell line at the highest concentration (Figure 6B & 6D). These data reveal F-4 to be a more potent inducer of G2/M arrest and apoptosis in PC-3 and LNCaP cell lines, respectively, compared to the N-terminal inhibitor 17-AAG.

Surface Plasmon Resonance (SPR) Analysis of F-4 Binding Hsp90

To demonstrate that Hsp90 specifically binds F-4, the interaction of F-4 with immobilized Hsp90 was measured by surface plasmon resonance (SPR) spectroscopy. Figure 7 (*panel A*) shows representative curves for the binding of F-4 to Hsp90. The binding of F-4 to Hsp90 was observed to be saturable (*panel B*) with a calculated K_d of 100 ± 10 μM and a stoichiometry of two moles per mole of Hsp90 chain. The plot of bound F-4 versus F-4 concentration gave a sigmoidal-like curve suggestive of cooperative binding. The Scatchard plot again suggested either cooperative binding of F-4 to Hsp90 or the presence of two binding sites with different affinities. A Hill plot of the data (*panel C*) yielded an IC_{50} for binding of 100 μM with a Hill coefficient of approximately two.

DISCUSSION

Hsp90 is a molecular chaperone required for the folding of nascent and denatured proteins. In the absence or inactivation of Hsp90, these client proteins are targeted for ubiquitination and proteasomal degradation. Though several N-terminal Hsp90 inhibitors have demonstrated client protein degradation, many of these agents have been hampered in clinical trials by high toxicity and poor solubility (19). The C-terminal ATP binding domain of Hsp90 is important for dimerization and can be inhibited by NB. We hypothesized that the targeting of Hsp90 by NB analogues would demonstrate a distinct mode of action compared to N-terminal inhibitors.

In this study we have demonstrated the effectiveness of a novel NB analogue, F-4, in comparison to 17-AAG. In anti-proliferation assays, F-4 demonstrates superior efficacy (IC_{90}) at 24 hours exposure compared to 17-AAG which requires 48–72 hours to achieve maximal response. A hallmark of Hsp90 inhibition is the degradation of client proteins; we therefore investigated the expression of client proteins previously established to be important in prostate cancer (20–22).

F-4 treatment of prostate cancer cells demonstrated that some client proteins such as HER-2 and AKT were affected across cell lines but another client, HIF-1α, was only affected in the PC-3 cell line. These data suggest that not all client proteins will be equally degraded following Hsp90 inhibition across prostate cancers. Interestingly, the induction of Hsp90, a hallmark of Hsp90 inhibition, is observed slightly in the PC-3 cell line and not at all in LNCaP cells. To date, it is unclear how Hsp90 induction will affect the clinical outcomes of N-terminal Hsp90 inhibitors. However, if this is proven to be undesirable, NB analogues targeting the C-terminal end of Hsp90 may offer distinct advantages in that they limit the

induction of Hsp90. Correspondingly, PSA levels decline at F-4 concentrations (10 μM) less than that required for cytotoxicity (25–100 μM), indicating that the reduction in PSA is a result of AR degradation and not cell death.

In studies examining cell cycle, induction of apoptosis and cytotoxicity of F-4 and 17-AAG, we note several key observations. First, F-4 appeared to have distinct effects on cell cycle causing LNCaP cells to shift into the sub-G0 apoptotic fraction and PC-3 cells to arrest in G2/M phase. Second, the LNCaP cell line is approximately two fold more sensitive to F-4 with respect to the induction of apoptosis and cytotoxicity compared to PC-3 cells. These observations, combined with the observed effects of F-4 on client proteins, suggest NB analogues may exert cell type-specific modes of action. Lastly, 17-AAG treatment of prostate cancer cells at concentrations up to 100 μM appeared to be largely cytostatic causing a G2/M arrest with mild induction of apoptosis in the LNCaP cell line and appreciable cytotoxicity seen only after 72 hours treatment.

Analysis of the binding of F-4 to Hsp90 by SPR indicated that Hsp90 binds F-4 specifically and cooperatively with a K_d of 100 μM, a binding affinity that is comparable to that previously reported for another novobiocin analogue, chlorobiocin (12). The Hill coefficient for the binding of F-4 to Hsp90 was approximately two, indicating that the binding was highly cooperative. The Hill coefficient is similar to that calculated for the binding of novobiocin to Hsp90, which is estimated from the concentration-dependent changes in Hsp90 conformation induced upon binding of Hsp90 to novobiocin (23).

CONCLUSIONS

The novobiocin analogue, F-4, is a putative C-terminal Hsp90 inhibitor with distinct pharmacodynamics compared to the N-terminal inhibitor 17-AAG. At equal concentrations, F-4 was demonstrated to be superior to 17-AAG at inducing apoptosis and causing cytotoxicity, and may offer distinct advantages over N-terminal inhibitors in the treatment of prostate cancer.

Acknowledgments

The authors gratefully acknowledge the support of this project by Department of Defense New Investigator Award, PC050629 of the Prostate Cancer Research Program, NIH (CA120458 and RO1CA125392), Project No. 1975 from the Oklahoma Agricultural Experiment Station. This work was supported in part by the Kansas Technology Enterprise Corporation through the Centers of Excellence Program. The authors would especially like to thank ICX Nomadics of Oklahoma for the loan of their SensiQ SPR Instrument. Finally, the authors would like to thank the other members of the Hsp90 Research Consortium, whose knowledge and expertise made this research possible: Roger A. Rajewski, John D. Robertson, Katherine F. Roby, and Len M. Neckers.

References

1. Jemal A, Tiwari RC, Murray T, Ghafoor A, Samuels A, Ward E, Feuer EJ, Thun MJ. Cancer statistics, 2004. CA Cancer J Clin. 2004; 54(1):8–29. [PubMed: 14974761]
2. Petrylak DP, Tangen CM, Hussain MH, Lara PN Jr, Jones JA, Taplin ME, Burch PA, Berry D, Moinpour C, Kohli M, Benson MC, Small EJ, Raghavan D, Crawford ED. Docetaxel and estramustine compared with mitoxantrone and prednisone for advanced refractory prostate cancer. N Engl J Med. 2004; 351(15):1513–1520. [PubMed: 15470214]
3. Tannock IF, de Wit R, Berry WR, Horti J, Pluzanska A, Chi KN, Oudard S, Theodore C, James ND, Turesson I, Rosenthal MA, Eisenberger MA. Docetaxel plus prednisone or mitoxantrone plus prednisone for advanced prostate cancer. N Engl J Med. 2004; 351(15):1502–1512. [PubMed: 15470213]

4. Stravopodis DJ, Margaritis LH, Voutsinas GE. Drug-mediated targeted disruption of multiple protein activities through functional inhibition of the Hsp90 chaperone complex. Curr Med Chem. 2007; 14(29):3122–3138. [PubMed: 18220746]
5. Neckers L. Heat shock protein 90: the cancer chaperone. J Biosci. 2007; 32(3):517–530. [PubMed: 17536171]
6. Chiosis G, Huezo H, Rosen N, Mimnaugh E, Whitesell L, Neckers L. 17AAG: low target binding affinity and potent cell activity--finding an explanation. Mol Cancer Ther. 2003; 2(2):123–129. [PubMed: 12589029]
7. Kamal A, Thao L, Sensintaffar J, Zhang L, Boehm MF, Fritz LC, Burrows FJ. A high-affinity conformation of Hsp90 confers tumour selectivity on Hsp90 inhibitors. Nature. 2003; 425(6956): 407–410. [PubMed: 14508491]
8. Sharp S, Workman P. Inhibitors of the HSP90 molecular chaperone: current status. Adv Cancer Res. 2006; 95:323–348. [PubMed: 16860662]
9. Marcu MG, Chadli A, Bouhouche I, Catelli M, Neckers LM. The heat shock protein 90 antagonist novobiocin interacts with a previously unrecognized ATP-binding domain in the carboxyl terminus of the chaperone. J Biol Chem. 2000; 275(47):37181–37186. [PubMed: 10945979]
10. Whitesell L, Shifrin SD, Schwab G, Neckers LM. Benzoquinonoid ansamycins possess selective tumoricidal activity unrelated to src kinase inhibition. Cancer Res. 1992; 52(7):1721–1728. [PubMed: 1551101]
11. Burlison JA, Blagg BS. Synthesis and evaluation of coumermycin A1 analogues that inhibit the Hsp90 protein folding machinery. Org Lett. 2006; 8(21):4855–4858. [PubMed: 17020320]
12. Galam L, Hadden MK, Ma Z, Ye QZ, Yun BG, Blagg BS, Matts RL. High-throughput assay for the identification of Hsp90 inhibitors based on Hsp90-dependent refolding of firefly luciferase. Bioorg Med Chem. 2007; 15(5):1939–1946. [PubMed: 17223347]
13. Yu XM, Shen G, Neckers L, Blake H, Holzbeierlein J, Cronk B, Blagg BS. Hsp90 inhibitors identified from a library of novobiocin analogues. J Am Chem Soc. 2005; 127(37):12778–12779. [PubMed: 16159253]
14. Burlison JA, Avila C, Vielhauer G, Lubbers DJ, Holzbeierlein J, Blagg BS. Development of novobiocin analogues that manifest anti-proliferative activity against several cancer cell lines. J Org Chem. 2008; 73(6):2130–2137. [PubMed: 18293999]
15. Goldson TMVG, Staub E, Miller S, Shim H, Hagedorn CH. Eukaryotic initiation factor 4E variants alter the morphology, proliferation, and colony-formation properties of MDA-MB-435 cancer cells. Molecular Carcinogenesis. 2007; 46(1):71–84. [PubMed: 17091471]
16. Son D, RKaTP. Tumor necrosis factor alpha (TNF) induces serum amyloid A3 in mouse granulosa cells. Endocrinology. 2004; 145:2245–2252. [PubMed: 14749357]
17. Grenert JP, Sullivan WP, Fadden P, Haystead TA, Clark J, Mimnaugh E, Krutzsch H, Ochel HJ, Schulte TW, Sausville E, Neckers LM, Toft DO. The amino-terminal domain of heat shock protein 90 (hsp90) that binds geldanamycin is an ATP/ADP switch domain that regulates hsp90 conformation. J Biol Chem. 1997; 272(38):23843–23850. [PubMed: 9295332]
18. Owen BA, Sullivan WP, Felts SJ, Toft DO. Regulation of heat shock protein 90 ATPase activity by sequences in the carboxyl terminus. J Biol Chem. 2002; 277(9):7086–7091. [PubMed: 11751892]
19. Zhang H, Burrows F. Targeting multiple signal transduction pathways through inhibition of Hsp90. J Mol Med. 2004; 82(8):488–499. [PubMed: 15168026]
20. Ayala G, Thompson T, Yang G, Frolov A, Li R, Scardino P, Ohori M, Wheeler T, Harper W. High levels of phosphorylated form of Akt-1 in prostate cancer and non-neoplastic prostate tissues are strong predictors of biochemical recurrence. Clin Cancer Res. 2004; 10(19):6572–6578. [PubMed: 15475446]
21. Isaacs JS, Xu W, Neckers L. Heat shock protein 90 as a molecular target for cancer therapeutics. Cancer Cell. 2003; 3(3):213–217. [PubMed: 12676580]
22. Mohler JL. A role for the androgen-receptor in clinically localized and advanced prostate cancer. Best Pract Res Clin Endocrinol Metab. 2008; 22(2):357–372. [PubMed: 18471792]

23. Yun BG, Huang W, Leach N, Hartson SD, Matts RL. Novobiocin induces a distinct conformation of Hsp90 and alters Hsp90-cochaperone-client interactions. Biochemistry. 2004; 43(25):8217–8229. [PubMed: 15209518]

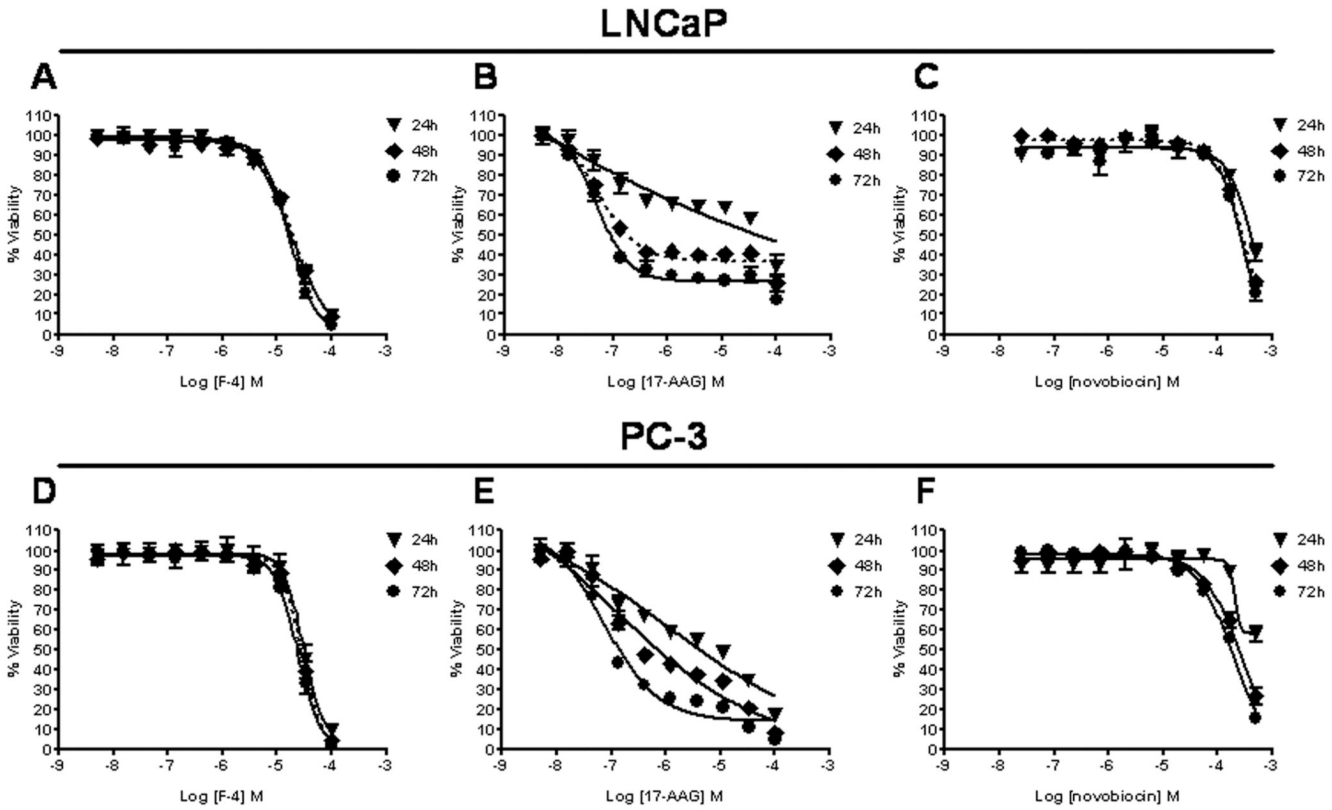

Figure One. Anti-proliferative effects of F-4 in prostate cancer cell lines

LNCaP *(top panels A–C)* and PC-3 cells *(bottom panels D–F)* were treated with F-4, 17-AAG, or novobiocin for 24(▼), 48(♦) and 72(●) hours. Bioreduction of tetrazolium (MTS) dye to a formazan by-product was used to measure cellular proliferation. Combined normalized data from independent experiments is shown for cells treated with F-4 (*panels A and D*), 17-AAG (*panels B and E*), and novobiocin *(panels C and F)*. Data was analyzed from 2–4 independent experiments performed in duplicate; each data point represents the mean ± SEM.

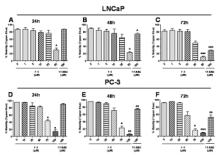

Figure Two. Cytotoxicity of F-4 in prostate cancer cells

LNCaP and PC-3 cells were treated with F-4 for 24, 48, and 72 hours. Samples were mixed with equal parts Trypan Blue and assessed for viability. Percentage viability was calculated as described in **Materials and Methods**. Asterisk(s) *, **, *** indicates significant *P value <0.05, <0.01, and <0.001*, respectively, by two-tailed t-test compared to vehicle-treated control.

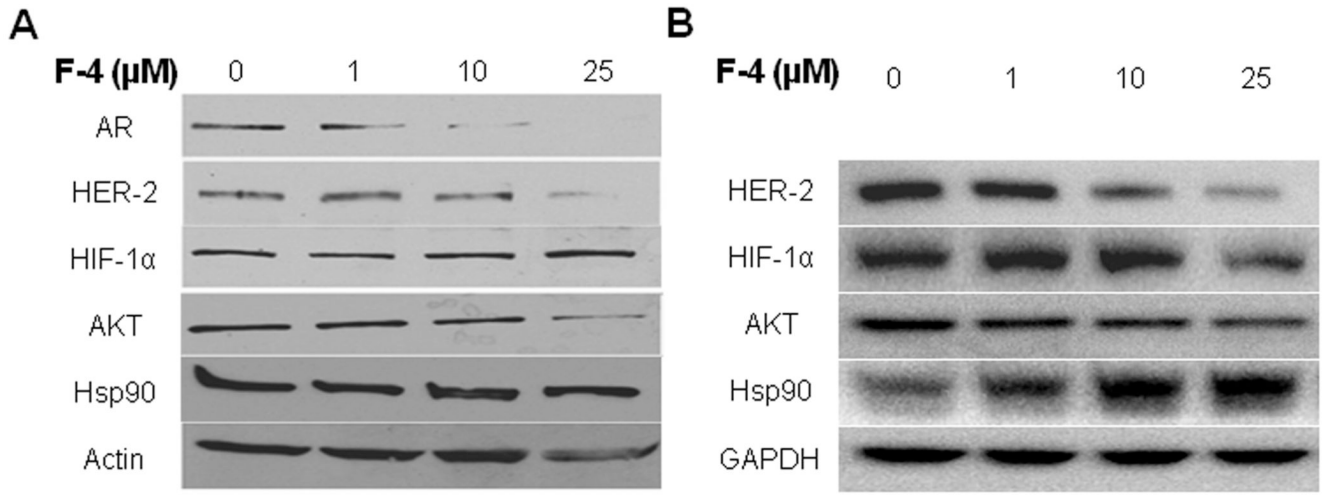

Figure Three. F-4 mediated degradation of client proteins

LNCaP (*panel A*) and PC-3 (*panel B*) cells were treated with F-4 then examined by Western blot for the degradation of client proteins. Actin (LNCaP) or GAPDH (PC-3) were used as loading controls for each panel.

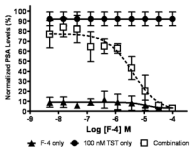

Figure Four. F-4 diminishes androgen induced PSA secretion

LNCaP cells were grown in hormone-free media for 72 hours, pre-treated with F-4 for 24 hours then were incubated either with F-4(▲), 100 nM testosterone (TST) (●), or in combination with F-4 (□). Data was analyzed from 4 independent experiments performed in duplicate; each data point represents the mean ± SEM for values obtained in the PSA ELISA assay.

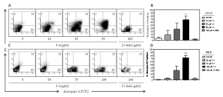

Figure Five. F-4 manifests induction of apoptosis in prostate cancer cells

LNCaP and PC-3 cells were treated with F-4 or 17-AAG for 72h. Representative flow cytometry scatterplots depict percent Annexin V staining for LNCaP *(panel A)* and PC-3 cells *(panel C)* after F-4 and 17-AAG treatment. The four quadrants of the scatterplot represent the percent of the parent population and indicate the following: *I*. PI- staining only indicating necrosis; *II*. Annexin V and PI staining depicting late-stage apoptosis; *III*. Negative staining indicating live cells; *IV*. Annexin V staining alone indicating early-stage apoptosis. A bar graph depicting the total percent apoptosis (Annexin V positive cells in quadrants II + IV) following treatment with statistical analysis is shown for LNCaP and PC-3 cells (*panels B and D, respectively*). Asterisk(s) *, ** indicates significant *P value <0.05, and <0.01*, respectively, by two-tailed t-test compared to vehicle-treated control.

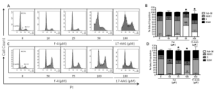

Figure Six. Cell cycle effects of F-4 in prostate cancer cells

Representative histograms are shown depicting the distribution of cell cycle as assessed by PI staining following treatment of LNCaP (*panel A*) and PC-3 (*panel C*) cells with F-4 or 17-AAG for 72h. Bar graphs depicting the cell cycle distribution after treatment from three independent experiments are shown with statistical analysis for LNCaP and PC-3 (*panels B and D, respectively*). Asterisk(s) *, ** indicates significant *P value <0.05 and <0.01*, respectively, by two-tailed t-test compared to vehicle-treated control.

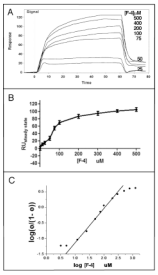

Figure Seven. Surface Plasmon Resonance (SPR) Analysis of F-4 Binding Hsp90

SPR analysis of the binding of F-4 to Hsp90 was carried out as described under **Materials and Methods.** *Panel A* demonstrates representative binding curves of F-4 injected at the indicated concentrations, while *panel B* displays replot of relative units at steady state ($RU_{steadystate}$: amount bound) versus concentration of F-4. *Panel C* displays a Hill plot of the binding of F-4 to Hsp90.

Table One

IC_{50} and IC_{90} values for anti-proliferative effects of F-4

IC_{50}, IC_{90}, and R^2 values were calculated from sigmoidal dose response curves generated as specified in **Materials and Methods**.

	LNCaP				PC-3			
DRUG	**TIMEPOINT**	**AVE. IC_{50} (μM)**	**AVE. IC_{90} (μM)**	**R^2**	**TIMEPOINT**	**AVE. IC_{50} (μM)**	**AVE. IC_{90} (μM)**	**R^2**
F-4	24h	18.18	97.08	0.969	24h	29.78	70.70	0.801
	48h	20.24	95.08	0.941	48h	28.12	70.86	0.939
	72h	16.65	54.95	0.960	72h	23.87	66.50	0.966
17-AAG	24h	^	^	^	24h	1.27	2505†	0.837
	48h	0.06	0.34	0.899	48h	0.12	107.80	0.900
	72h	0.05	0.23	0.901	72h	0.08	0.94	0.962
Novobiocin	24h	436.10	1445†	0.883	24h	201.80	254.20	0.730
	48h	293.70	980.80	0.966	48h	252.50	1388†	0.963
	72h	274.10	785.00	0.909	72h	181.30	1007†	0.976

The symbol ^ indicates inability to generate IC_{50} and IC_{90} due to the failure of 17-AAG to generate a dose-response curve at this timepoint, and the symbol † identifies extrapolated IC_{50} and IC_{90} values from the dose response curve. Data was analyzed from 2–4 independent experiments performed in duplicate.